Advanced modeling of embedded piezo-electric transducers for the health-monitoring of layered structures

Advanced modeling of embedded piezo-electric transducers for the health-monitoring of layered structures

Enrico Zappino[a]* and Erasmo Carrera[a]

[a]*Mul2 Research Group, Department of Mechanical and Aerospace Engineering, Politecnico di Torino, Corso Duca degli Abruzzi 24, 10129 Torino, Italy.*

*enrico.zappino@polito.it

Advanced modeling of embedded piezo-electric transducers for the health-monitoring of layered structures

The present paper presents an innovative approach for the numerical modeling of piezo-electric transducers for the health-monitoring of layered structures. The numerical approach has been developed in the frameworks of the Carrera Unified Formulation. This computational tool allows refined numerical models to be derived in a unified and efficient fashion. The use of higher-order models and the capability to connect different kinematic models using the node-dependent kinematic approach has led to an efficient modeling technique for global-local analysis. This approach can refine the model only in those regions where it is required, e.g., the areas where piezo-electric transducers are placed. The model has been used to study embedded and surface-mounted sensors. The accuracy of the present model has been verified by comparing the current results with numerical and experimental data from the literature. Different modeling solutions have been developed, mixing one-, two- and three-dimensional finite elements. The results show that the use of the present modeling technique allows the computational cost to be reduced with respect to the classical approaches preserving the accuracy of the results in the critical areas.

Introduction

The prediction of the failure of composite structures and their health-monitoring are critical factors in the design of the next generation light-weight structures. The use of sensor networks can provide a large amount of data that can be processed and used to predict the residual structural integrity (1,2).

In the last decades, many research projects and industrial applications have been focused on the use of piezoelectric materials as sensors for the identification of structural damage (3). Piezoelectric materials have the property to originate an electric field as a consequence of a mechanical load and, at the same time, they generate mechanical strains when they are subject to an electric field. The design of piezoelectric devices requires the solution of an electro-mechanical coupled problem in which the electric potential becomes one of the primary variables of the problem (4).

The sensing capabilities of piezoelectric sensors have been widely used for active and passive monitoring of laminated structures (5,6). The sensing devices can be applied on the surface of the structure to be monitored (7,8) or they can be embedded (9) in the hosting structure. Figure 1 shows the two strategies. The use of surface-mounted sensors eases the installation of these devices on new or existing structures but keeps the sensors exposed to external agents.

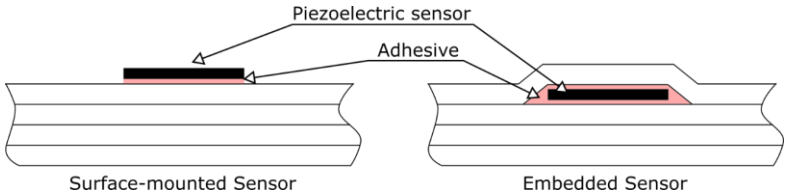

Figure 1 Example of surface-mounted and embedded piezoelectric sensors.

Embedded sensors can be installed in laminated structures, e.g., composite materials, during the manufacturing process. The use of embedded sensors leads to a higher sensitivity of the devices since they are strongly bonded to the hosting structure (10) and give to the sensor certain protection. On the other hand, the manufacturing of composite material with embedded sensors (11,12) can be challenging since the curing temperature must not exceed the Curie temperature of the active material. Moreover, the use of integrated sensors can produce local defects and stress concentrations that reduce the performances of the hosting structure (13). Dedicated manufacturing techniques, e.g. the interlacing (14), have been proposed to minimize the local impact of the sensor (15). An alternative to the use of localized piezo patches is represented by the use of embedded piezo fibers, an example is shown in (16).

Proper numerical modeling techniques can be used to predict the performances of active structures with embedded devices, preserving their integrity. In the last decades, many research papers have been presented on the modeling of smart structures

(4,17). Classical one- and two-dimensional structural models are inaccurate when they are used in the analysis of smart structures since their fundamental assumptions do not allow complex stress and strain fields to be predicted. The use of three-dimensional models can lead to accurate results but requires a huge computational cost. The constraints on the solid element aspect-ratio and the small thickness of the active layers, require refined meshes to be used to preserve the model accuracy.

The use of an iso-geometric approach for the optimization of micro and nanostructures of flexoelectric materials has been proposed in (18). The solution of an inverse-problem (19) has been demonstrated to be able to detect voids and inclusions in piezoelectric materials.

The use of higher-order finite elements for the analysis of smart structures have been proposed in many works (20) (21). The capabilities of these models have been often used to predict the free vibration of panels with piezo patches (22) or to predict the damping capabilities of active control systems (23). Three-dimensional exact solutions of piezoelectric layered structures have been presented by Kulikov and Plotnikova (24). The use of sinus finite elements has been proposed in (25) to avoid the use of shear correction factors in the analysis of laminated structures with distributed piezoelectric layers.

Carrera and his research group proposed the use of a unified formulation for the development of refined models for smart structures (26,27) considering also mixed formulations (28). The use of refined models can lead to accurate results, but it still requires a high computational cost if large structures are considered.

A reduction in the computational cost can be achieved by implementing global-local modeling techniques that make it possible to refine the solution locally. An example of these approaches is based on the use of transitional elements (29) that can

connect a global plate model to a local model based on solid elements. Srivastava and Lanza di Scalea (30) and Spada *et al.* (31) proposed a global-local approach where the finite element (FE) and a Semi-Analytical FE (SAFE) are used to investigate the integrity of composite structures. A global-local approach based on FEM/BEM (Boundary Element Method) analysis has been proposed in (32) to investigate damaged aircraft structures.

The aim of this article is to present an advanced global-local modeling technique for the analysis of surface-mounted and embedded piezoelectric transducers based on the Carrera Unified Formulation (33). This numerical tool can be used to derive any order structural models in a unified fashion. Recently, the formulation has been extended to multidimensional models (34) and, thanks to the node-dependent kinematic, NDK, formulation (35) the order of expansion of the structural model can be considered as a property of the node (36). These capabilities have originated a powerful framework for global-local analysis (37) since the numerical model can be refined only in those areas of the structure where complex phenomena are expected. An application of the NDK formulation to piezo-electric beams can be found here (36). In the present work, these techniques have been extended at the analysis of surface-mounted and embedded piezoelectric sensors as the basis for the design of health-monitoring system.

In the first part of the article, the Carrera Unified Formulation and the related modeling techniques are presented. In the second part, the present approach is used to investigate and compare two structures, the first with a surface-mounted sensor and the latter with an embedded transducer. The results have been compared with those from numerical and experimental analysis proposed in the literature.

Computational Model

This section introduces the numerical model used in the present paper. An overview of the Carrera Unified Formulation and of the structural theories adopted is reported. Afterward, the modeling techniques for the case of embedded and surface-mounted sensors are presented.

Preliminaries

The solution of the coupled electro-mechanical problem requires to consider the electric potential, ϕ, as a primary variable of the problem. The generalize displacement, $\boldsymbol{q}$, vector can be written as:

$$\boldsymbol{q} = \{u_x \quad u_y \quad u_z \quad \phi\}^T, \tag{1}$$

and the electric field vector, $\boldsymbol{E}$, can be written as:

$$\boldsymbol{E} = \{E_x \quad E_y \quad E_z\}^T = \{\partial_x \quad \partial_y \quad \partial_z\}^T \phi\,. \tag{2}$$

The generalized strain vector, $\bar{\varepsilon}$, can be written as:

$$\bar{\boldsymbol{\varepsilon}} = \{\varepsilon_{xx} \quad \varepsilon_{yy} \quad \varepsilon_{zz} \quad \varepsilon_{xz} \quad \varepsilon_{yz} \quad \varepsilon_{xy} \quad \mathrm{E}_x \quad \mathrm{E}_y \quad \mathrm{E}_z\}^T = \boldsymbol{Dq}; \tag{3}$$

where $\boldsymbol{D}$ is the matrix of the differential operators. The complete form of the matrix can be found in (36).

The electromechanical constitutive equations can be expressed as follows:

$$\begin{aligned} \boldsymbol{\sigma} &= \boldsymbol{C\varepsilon} - \boldsymbol{e}^T\boldsymbol{E}; \\ \boldsymbol{D_e} &= \boldsymbol{e\varepsilon} + \boldsymbol{\chi E}, \end{aligned} \tag{4}$$

where $\mathbf{D_e}$ is the electric displacement vector $\{\mathrm{D_x}, \mathrm{D_y}, \mathrm{D_z}\}^{\mathrm{T}}$, and $\boldsymbol{\sigma}$ is the mechanical stress vector, $\mathbf{C}$ the matrix of mechanical material coefficients. $\boldsymbol{\chi}$ is the dielectric permittivity matrix. The piezoelectric stiffness coefficients are stored in matrix **e.**

The generalized stress vector can be arranged as:

$$\bar{\boldsymbol{\sigma}} = \{\sigma_{xx} \quad \sigma_{yy} \quad \sigma_{zz} \quad \sigma_{xz} \quad \sigma_{yz} \quad \sigma_{xy} \quad \mathrm{D}_x \quad \mathrm{D}_y \quad \mathrm{D}_z\}^T. \tag{5}$$

The generalized stress vector can be obtained as:

$$\bar{\boldsymbol{\sigma}} = \boldsymbol{H}\bar{\boldsymbol{\varepsilon}}\,. \tag{6}$$

Kinematic assumptions

The three-dimensional generalized displacement field can be written in the general form as:

$$\boldsymbol{q} = \boldsymbol{q}(\mathbf{x}, \mathbf{y}, \mathbf{z}) \tag{7}$$

When slender bodies must be investigated it is justified to reduce the three-dimensional problem to an one-dimensional problem. In this case, the generalized displacement field can be written as:

$$\boldsymbol{q^{1D}} = \mathrm{F}_\tau(x, z)\boldsymbol{q}_\tau(y) \tag{8}$$

Where the $F_\tau(x, z)$ is the functions expansion used to approximate the cross-sectional kinematic of the one-dimensional model. $\boldsymbol{q}_\tau(y)$ are one-dimensional unknown functions. The index τ denotes the term of the expansion.

The choice of the expansion generates different kinematic models, the use of a Taylor expansion leads to equivalent single layer (ESL) models while, when Lagrange functions are used, layer-wise (LW) models can be obtained. More details can be found in (25).

The analysis of thin structures can be carried out introducing two-dimensional models, in this case Eq. (7) becomes:

$$\boldsymbol{q^{2D}} = \mathrm{F}_\tau(z)\boldsymbol{q}_\tau(x, y) \tag{9}$$

The kinematic approximation is introduced through-the-thickness by means of the expansion F_τ, while the unknow quantities $\mathbf{q}_\tau$ are defined on the reference plane of the structure. The structural model depends on the kinematic approximation used, as for the case of the one-dimensional models, a Taylor expansion leads to ESL models while Lagrange functions can be used to derive LW models.

The solution of the problem can be obtained using the classical finite element formulation, that is, a set of shape functions, $\mathrm{N_i}$, can be use do approximate the one-, two- or three-dimensional problem.

The final formulation of the generalized displacement field for the three cases can be written as:

$$\begin{aligned} \boldsymbol{q^{3D}} &= \mathrm{N_i}(x,y,z)\boldsymbol{q_i} \\ \boldsymbol{q^{2D}} &= \mathrm{N_i}(x,z)\mathrm{F_\tau^i}(z)\boldsymbol{q_{i\tau}} \\ \boldsymbol{q^{1D}} &= \mathrm{N_i}(y)\ \mathrm{F_\tau^i}(x,z)\boldsymbol{q_{i\tau}} \end{aligned} \tag{10}$$

The index *i* on the F_τ comes from the node dependent kinematic approach, NDK, and denotes that for each node $\boldsymbol{i}$ a different kinematic assumption can be introduced.

Node-dependent kinematic models

The NDK approach is used, in the present paper, to refine locally the numerical model and to impose compatible kinematic models at the interface between one- two- and three-dimensional elements. The theoretical derivation of the NDK modeling approach has been presented in (35) and has been used for the analysis of piezoelectric structure in (36). A simple, two node, beam element is here used to present the approach.

The displacement field of the considered beam model can be written as follow:

$$\boldsymbol{q^{1D}} = \mathrm{N_1}(y)\ \mathrm{F_\tau^1}(x,z)\boldsymbol{q_{1\tau}} + \mathrm{N_2}(y)\ \mathrm{F_\tau^2}(x,z)\boldsymbol{q_{2\tau}} \tag{11}$$

Where $\mathrm{N_1}$is the shape function in node 1 while $\mathrm{N_2}$ is the shape function of node two. In each node a different kinematic model can be imposed, here a first order Taylor expansion is considered at the first node:

$$\mathrm{F_\tau^1}(x,z) = 1q_{11} + \mathrm{x}\,q_{12} + \mathrm{z}\,q_{13}\,; \tag{12}$$

while a four-node linear Lagrange expansion, L_τ, is used on the cross-section placed on node 2:

$$F_\tau^2(x,z) = L_1 q_{21} + L_2 q_{22} + L_3 q_{23} + L_4 q_{24}. \quad (13)$$

The displacement filed of the element thus is:

$$\boldsymbol{q^{1D}} = N_1(1 q_{11} + x\, q_{12} + z\, q_{13}) + N_2\,(L_1 q_{21} + L_2 q_{22} + L_3 q_{23} + L_4 q_{24}). \quad (14)$$

Governing equation

The stiffness matrix, as well as the external load vector, can be derived by applying the principle of virtual displacement (PVD). By substituting the constitutive equations, the following expression can be attained:

$$\boldsymbol{\delta L_{int}} = \int_V \boldsymbol{\delta}\, \bar{\varepsilon}^T \bar{\sigma}\, \boldsymbol{dV} = \boldsymbol{\delta L_{ext}} \quad (15)$$

If the geometrical relations and shape functions are substituted into the above expression, one can obtain:

$$\boldsymbol{\delta L_{int}} = \delta \mathbf{q}_{sj} \int_V N_j \mathbf{I}\, F_s^j \mathbf{D}^T \mathbf{H} \mathbf{D} F_\tau^i \mathbf{I} N_i dV \mathbf{q}_{i\tau} \quad (16)$$

in which I is a 4x4 identity matrix. In a more compact form, the above expression can be written as:

$$\delta L_{int} = \delta \mathbf{q}_{sj}^T \mathbf{K}_{ij\tau s} \mathbf{q}_{\tau i} \quad (17)$$

where $\mathbf{K}_{ij\tau s}$ is the fundamental nucleus of the stiffness matrix. The global stiffness matrix can be obtained by the proper assembly of fundamental nuclei evaluated for each combination of the indexes i, j, τ, and s. More details about the assembly procedure can be found in (25).

Global-local modeling techniques

Figure 2 shows an example of an aeronautical reinforced structure with two sensors embedded in the panels. Despite classical finite element formulations have been used over the years to analyze such thin-walled structures, these models are not effective in the prediction of the local effects originated by the sensors. The investigation of the output of the sensors resulting from a structural deformation requires a coupled analysis where both mechanical and electrical fields must be defined. The local response can be highly three-dimensional, that is, solid element are often used to solve the multifield problem locally.

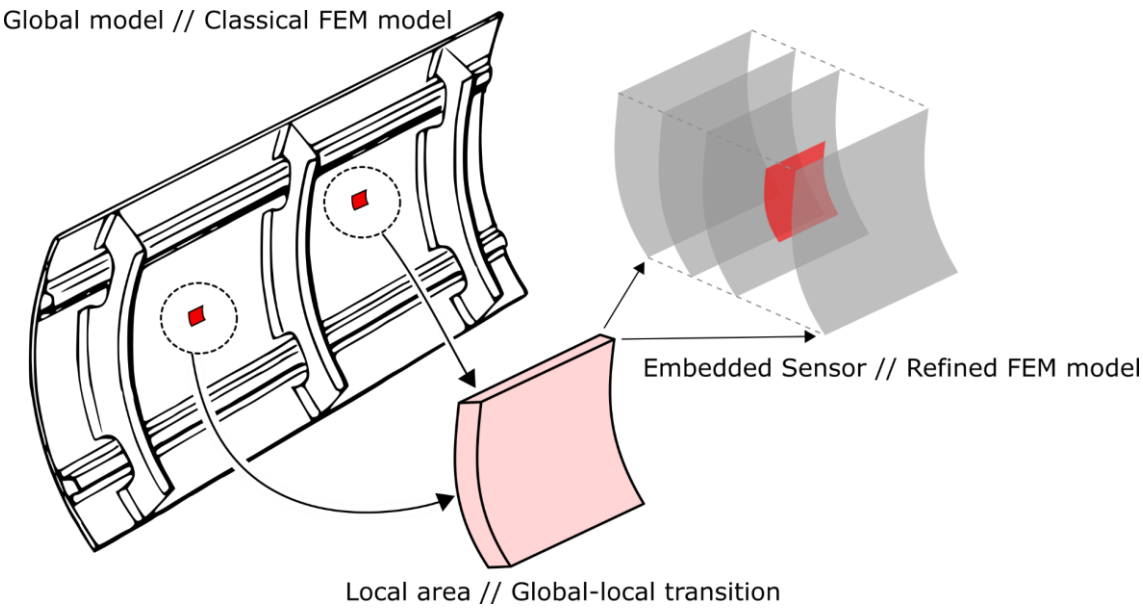

Figure 2 Example of an aeronautical structure with embedded piezoelectric sensors.

The coupling of refined local and coarse global models has been the topic on many research works (38,39) and has been solved mainly using transitional elements (29) or imposing *ad hoc* constrains at the interface of the local and the global model, e.g. using Lagrange multipliers.

This section presents an advanced technique for the global-local modelling of smart structures that takes advantage of the capabilities of the Carrera Unified Formulation to derive any order theories with a systematic procedure. The local refinement of the model and the transition between elements with different dimensions can be achieved using the NDK approach.

Figure 3 shows an example of a plate with an embedded sensor. The use of a 2D LW model in the sensor area ensures high accuracy of the results. The transition area between the sensor and the hosting structure can have a variation in the thickness of the structure, in this case, three-dimensional elements can be used to ensure a high-fidelity representation of the geometry. Finally, classical two- and one-dimensional models can be used for the hosting structure where no complex phenomena are expected.

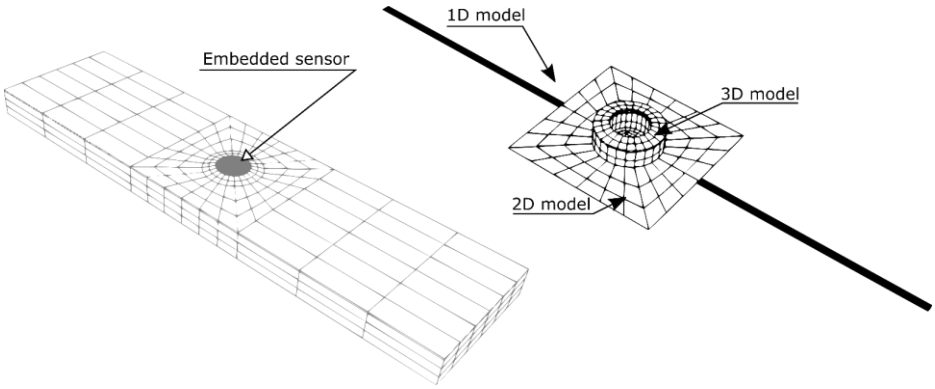

Figure 3 Example of the global-local modeling of a structure with an embedded piezo-sensor.

The transition strategies between models with different dimension are shown in Figure 4. Using the NDK approach, it is possible to impose compatible kinematic models at the interface between elements with different dimensions (37).

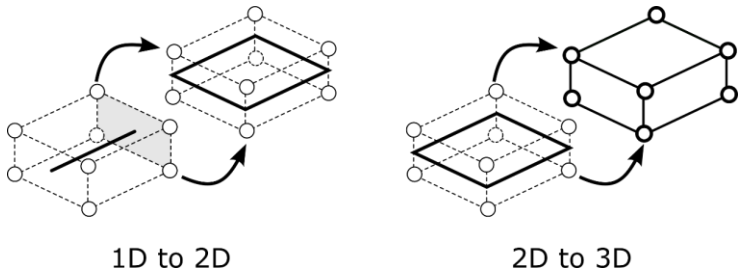

Figure 4 Transition strategy between 1D and 2D models and between 2D and 3D models (34) .

The use of kinematic models based on Lagrange functions originates a formulation with only displacements as degrees-of-freedom, that is, one-, two- and three-dimensional elements can be easily connected by imposing the equivalence of the displacements at the shared nodes (34).

Numerical Results

Two specimens, one with a surface-mounted sensor and one with an embedded transducer are considered in this section. The two benchmarks came from the work by Shin *et al.*(10) where numerical and experimental results have been presented.

The specimens have been built using glassfiber-epoxy composite with a stacking sequence equal to $[0/90]_{10S}$, both have a piezoelectric circular transducer serving as a sensing device, the transducer is considered bounded with an adhesive. The laminate, piezoelectric material and adhesive properties are reported in *Table 1*.

Material	Fiberglass/epoxy	PZT-5A	Adhesive
E_L (GPa)	20.1	61.0	1
E_T (GPa)	21.8	61.0	1
E_Z (GPa)	12.7	53.2	1
ν_{LT}	0.115	0.35	0.35
ν_{LZ}	0.212	0.384	0.35
ν_{ZT}	0.452	0.384	0.35
G_{LT} (GPa)	3.8	21.1	0.37
G_{LZ} (GPa)	7.6	21.6	0.37
G_{ZT} (GPa)	7.5	22.6	0.37
e_{31} (C/m^2)	-	-5.35	-
e_{15} (C/m^2)	-	12.29	-
e_{33} (C/m^2)	-	15.78	-
$\varepsilon_{11}^*/\varepsilon_0$	-	919	-
$\varepsilon_{33}^*/\varepsilon_0$	-	914	-
ρ (kg/m^3)	1896	7800	1200

*Constant strain

Table 1 Material properties used in the simulation (ε_0 is the permittivity in the free space)

The geometry of the two specimens is reported in Figure 5 Geometry of the models considered**.** The point P denotes the position in which the axial strain has been evaluated, via strain gauge, during the test and is placed at 8 mm from the halfwidth of the specimen. The surface-mounted sensor is considered bounded at the coupon surface via a layer of adhesive with a thickness of 0.15 mm. The piezoelectric sensor has a circular shape with a diameter of 6.3 mm and a thickness of 0.191 mm.
The embedded sensor is placed under the upper glassfiber ply, which has with a thickness of 0.00027, and is bounded with a layer of adhesive all around the sensor. The details of the piezo transducers are shown in Figure 6.

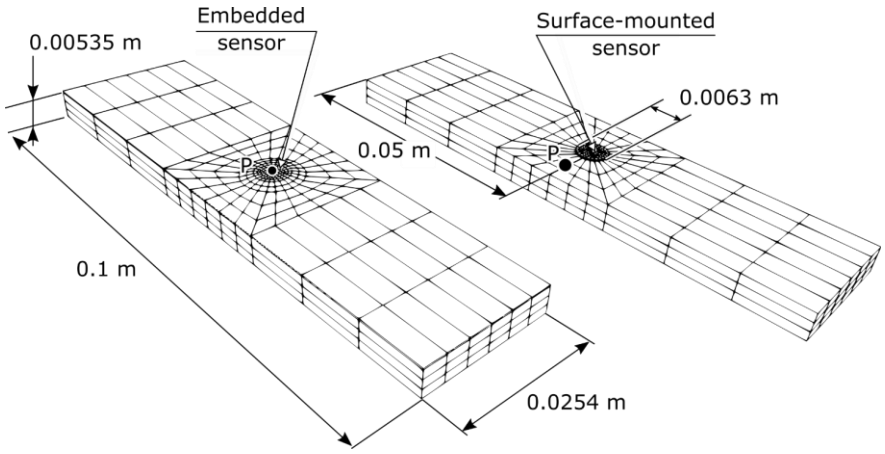

Figure 5 Geometry of the models considered

A three-point bending test has been simulated imposing a vertical displacement of 1mm at the center of the specimens. The response in terms of voltage and strain have been evaluated and compared with those reported in the literature. Figure 7 shows the details of the virtual test setup and the reference system used in the analysis. The two lateral supports have been modeled as simply support boundaries.

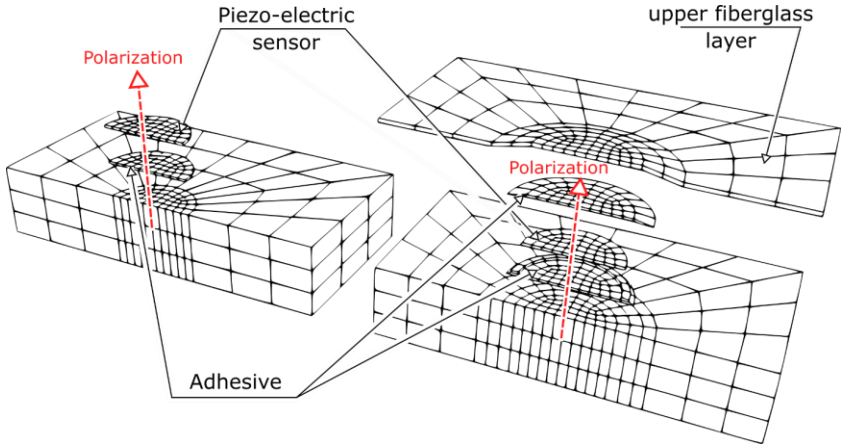

Figure 6 Details of the sensor area for the surface mounted (left) and embedded (right) sensors.

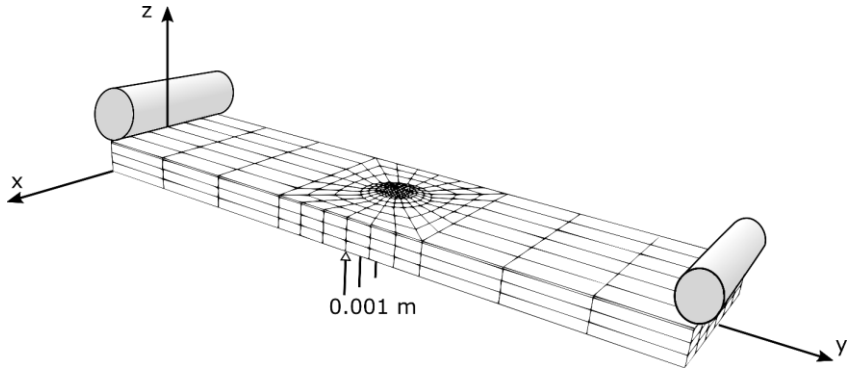

Figure 7 Virtual test setup and reference system for the embedded sensor specimen. The same setup has been used for the surface-mounted sensor coupon.

Different modeling approaches have been used to investigate the static and electro-mechanical response of the structures. Figure 8 shows the subdivision of the structure with the embedded sensor in different subdomains or areas, each of them can be analyzed with a different kinematic. The same subdivision has been adopted for the specimen with the surface-mounted sensor unless subdomain 4, in this case, subdomain 2 is directly connected with subdomain 5.

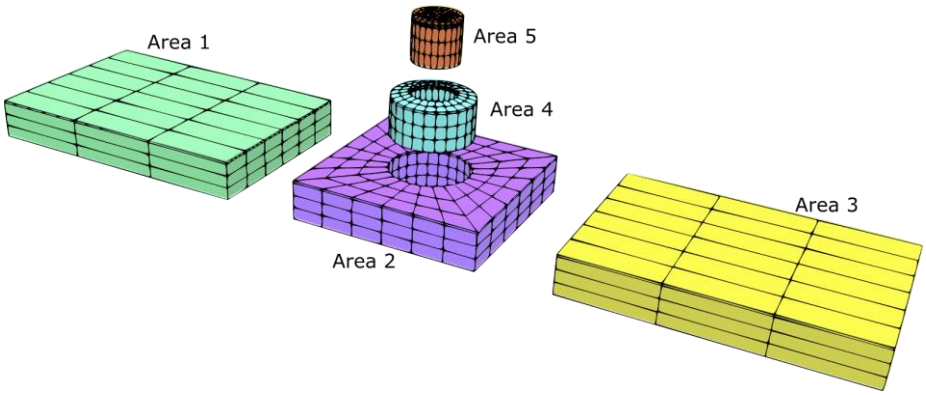

Figure 8 Subdivision of the specimen in different subdomains each of them can have a different kinematic.

*Table 1*Table 2 shows the different combinations of kinematic models considered. Models EMB-1 to EMB-4 are related to the embedded sensor specimen while models SUR-1 to SUR-4 are related to the surface-mounted sensor coupon.

Two different plate models have been considered. The TE-2 model uses a quadratic Taylor expansion through-the-thickness of the plate and is based on an equivalent single layer approach. The LE model is a layer-wise model based on Lagrange functions, in this case three quadratic elements have been used through-the-thickness of hosting structure, additional elements have been added to include the adhesives and the piezo patch.

	Area 1	Area 2	Area 3	Area 4	Area 5	DOFs
EMB-1	2D (TE-2)	2D (TE-2)	2D (TE-2)	2D (TE-2)	2D (TE-2)	7245
EMB-2	2D (LE)	2D (LE)	2D (LE)	3D	2D (LE)	38313
EMB-4	2D (TE-2)	2D (LE)	2D (TE-2)	3D	2D (LE)	30753
EMB-4	1D (TE-2)	2D (LE)	1D (TE-2)	3D	2D (LE)	29781
SUR-1	2D (TE-2)	2D (TE-2)	2D (TE-2)	-	2D (TE-2)	7245
SUR -2	2D (LE)	2D (LE)	2D (LE)	-	2D (LE)	22320
SUR -3	2D (TE-2)	2D (TE-2)	2D (TE-2)	-	2D (LE)	17691
SUR -4	1D (TE-2)	2D (LE)	1D (TE-2)	-	2D (LE)	17046

Table 2 Elements (3D -solid; 2D – plate; 1D – beam) and Kinematic models (TE- Taylor expansion; LE – Lagrange expansion) considered for each subdomain.

A second order beam model, 1D (TE-2), has been used in the subdomain 1 and 3 where no local effects were expected. A Lagrange Expansion, LE, beam model has been used at the interface between beam and plate models to obtain the displacement continuity. A standard quadratic kinematic was considered when solid elements have been employed, that is, 27-node solid elements have been adopted.

Surface-mounted sensor analysis

The results for the surfaced mounted sensor specimen are presented in this section. At first, a static analysis has been carried out to investigate the effects of the modeling approaches on the strain and stress distributions. Then, the coupled electro-mechanical problem has been solved to investigate the electric response originated by the applied displacement.

Static Analysis

The results coming from the static analysis are reported in Table 3. The first column reports the modeling approach while columns two and three show the axial strain and stress evaluated at the central point of the piezo transducer. The results show that the use of a full equivalent single layer model, model SUR-1, leads to an overestimation of the axial strain and stress if compared with a full LW approach, model SUR-2.

Model	ε_{yy}	σ_{yy} [MPa]
SUR-1	0.002243	168.78
SUR -2	0.001455	89.91
SUR -3	0.001465	90.27
SUR -4	0.001452	89.69

Table 3 Axial Stress and strain evaluated at the center of the piezo patch using different modeling approaches.

Models SUR-3 and SUR-4 can replicate the solution of the layer-wise model using an accurate kinematic approximation only in the sensor area.

The lack of accuracy showed by model SUR-1 can be explained by looking at the results in Figure 9. The picture reports trough-the-thickness distributions of the axial strain and stress evaluated in the central point of the sensor. Only the upper part of the specimen (0.003 mm < z < top) has been reported to emphasize the sensor area.

The results show that an ESL approach is unable to detect the discontinuities in the strain field originated by the interfaces between the substrate and the adhesive, and between the adhesive and the piezo transducer. Consequently, the axial stress predicted in the active material is much larger than expected, almost the double.

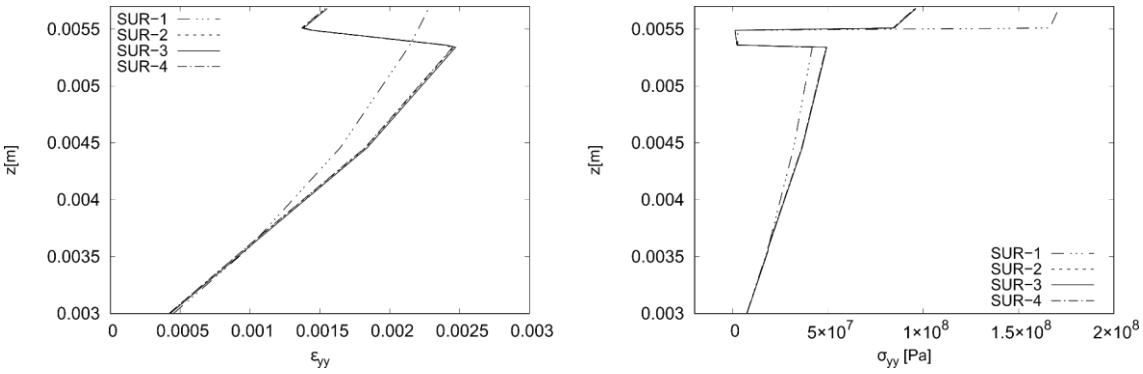

Figure 9 Axial strain, on the left, and stress, on the right, distribution through-the-thickness. The results have been evaluated in the central point of the piezo transducer.

Electro-mechanical Analysis

The lack of accuracy of model SUR-1 in the prediction of the static response of the structure can be also seen in the results of the coupled electro-mechanical analysis.

Table 4Table 4 Electro-mechanical coupled analysis of the surface-mounted sensor specimen. Axial strain, voltage, and effective coupling factor. reports the axial strain evaluated at points P, see Figure 5, the voltage generated by the deformation and the ratio between these two quantities that denotes the effective coupling factor. The results

are compared with those from literature (10) where experimental and numerical results have been presented. The use of ESL models for the description of the electric potential is not recommended since it has a typical piece-wise distribution. In the present work the electric potential for model SUR-1 has been evaluated starting from the axial strain distribution following the procedure presented in (40).

Model	ε_{yy}	V	V/ ε_{yy} [V/με]
Experimental (10)	-	-	0.036
3D FEM (10)	-	-	0.036
SUR-1	0.00291	175.5 †	0.060
SUR -2	0.00307	108.6	0.035
SUR -3	0.00300	108.1	0.036
SUR -4	0.00308	108.3	0.035
SUR -2*	0.00299	188.0	0.063

† The electric potential has been evaluated using the formulation in (40)

Table 4 Electro-mechanical coupled analysis of the surface-mounted sensor specimen. Axial strain, voltage, and effective coupling factor.

As expected, the model SUR-1 is unable to predict the correct response overestimating the effective coupling factor. The prediction of a higher coupling is due to the fact that, an equivalent single layer approach cannot describe the interface between the hosting structure and the piezo-electric transducer properly. The lower stiffness of the adhesive reduces the coupling between the two joined components that is, the piezo patch cannot see the same strain of the structure. To confirm this results model SUR -2* has been introduced. This model is equivalent to model SUR-2 but the adhesive has a stiffness 100 times higher, that is, a perfect bonding is ensured. In this case, the value of the effective coupling factor is much closer to the value provided by model SUR-1.

The use of variable kinematic models, SUR-2 and SUR-4, allows to achieve the same results of the full layers-wise model with a reduced computational cost. *Table 5* shows the reduction of the computational costs achieved using the present variable kinematic models.

Despite the number of degree of freedom in the area 5, see Figure 8 Subdivision of the specimen in different subdomains each of them can have a different kinematic. is constant, the use of a reduced-order model elsewhere can provide a computational cost saving in areas 1 to 4 up to 56%.

Model	$DOF^{\text{Full model}}$	$DOF^{\text{Area 5}}$	$DOF^{\text{Area 1-4}}$	$\Delta\%\ DOF^{\text{Area 1-4}}$
SUR -2	22320	12996	9324	-
SUR -3	17691	12996	4695	-49.6
SUR -4	17046	12996	4050	-56.6

Table 5 Computational cost reduction using variable kinematic models.

Embedded sensor analysis

In this section are reported the results obtained considering the specimen with the embedded sensor. Both static and coupled electro-mechanical analyses have been performed.

Static Analysis

The results obtained through a static pure mechanical analysis have been reported in Table 6.

The axial strain, as well as the axial stress, have been evaluated at the center of the piezo transducer. The results confirm the outcome of the previous case. The use of an equivalent single layer model, EMB-1, leads to inaccurate results since it is not able to predict the interface between the active material and the hosting structure properly. Variable kinematic models, EMB-3 and EMB-4, provide accurate results with a lower number of degrees of freedom with respect to the refined model, EMB-2.

Model	ε_{yy}	σ_{yy} [MPa]
EMB-1	0.002141	164.56
EMB-2	0.001790	115.22
EMB -3	0.001801	116.70
EMB-4	0.001792	116.12

Table 6 Axial Stress and strain evaluated at the centre of the piezo patch using different modeling approaches.

Figure 10 shows through-the-thickness distributions of the axial strain and stress at the central point of the piezo transducer. The results show that EMB-1 is not able to predict the piece-wise distribution of the strain and, as a consequence, this model provides an inaccurate distribution of axial stress, mainly in the piezo sensor.

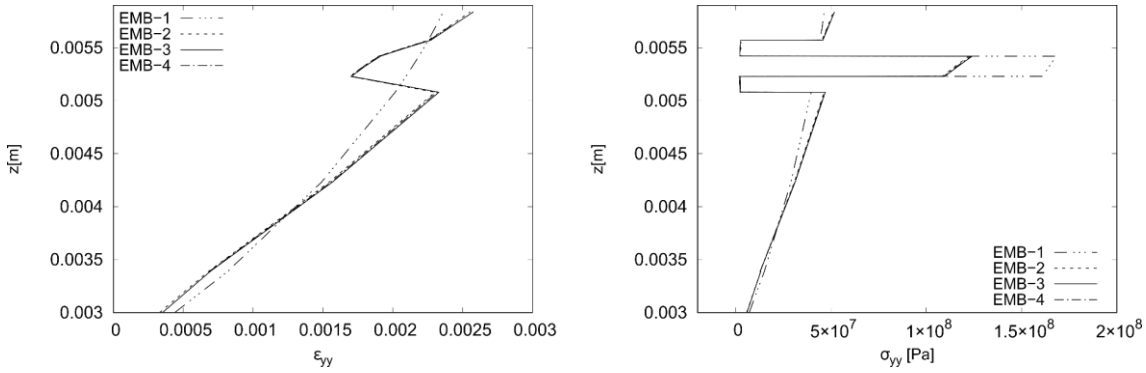

Figure 10 Axial strain, on the left, and stress, on the right, distribution through-the-thickness of the embedded sensor specimen. The results have been evaluated in the central point of the piezo transducer

Electro-mechanical Analysis

The results of the coupled electro-mechanical analysis are reported in Table 7. The results have been compared with those from literature (10).

All the models, except EMB-1, predict the expected value of effective coupling factor, that is, a correct description of axial strain, evaluated at point P, and voltage is obtained. Model EMB-1 shows the limits of the ESL formulation. The coarse description of the interface between the piezo and the substrate leads to an overestimation of the voltage and, as a consequence, the effective coupling factor is greater than the reference value.

Model	ε_{yy}	V	V/ ε_{yy} [V/με]
Experimental (10)	-	-	0.086
3D FEM (10)	-	-	0.081
EMB-1	0.002361	272.18†	0.115
EMB-2	0.002488	216.25	0.087
EMB-3	0.002509	222.01	0.088
EMB-4	0.002496	220.80	0.088

† The electric potential has been evaluated using the formulation in (40)

Table 7 Electro-mechanical coupled analysis of the embedded sensor specimen. Axial strain, voltage, and effective coupling factor.

The use of an ESL model also introduces some approximations in the description of the geometry of the coupon.

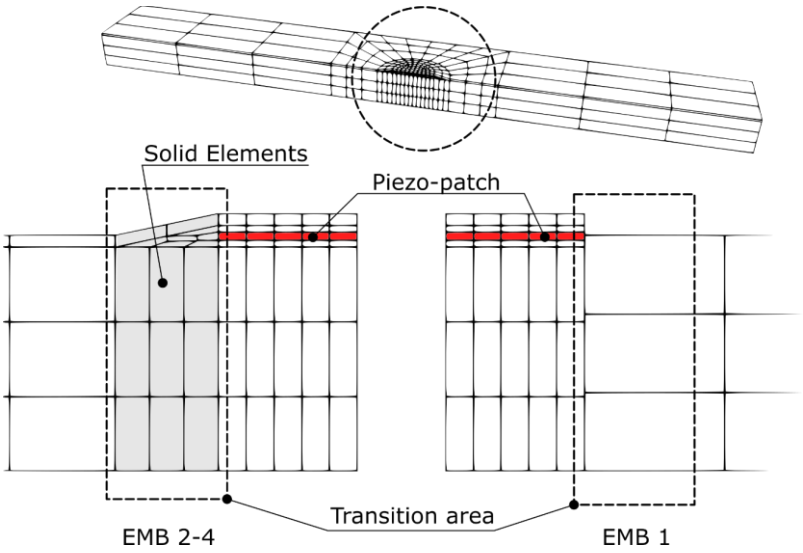

Figure 11 Details of the area around the piezo patch. The use of solid elements in models EMB 2-4 leads to a high-fidelity representation of the geometry while model EMB-1 introduces some simplifications.

Figure 11 shows the details of the transition between the area of the piezo patch and the surrounded structure. The use of solid elements in models EMB-2 to EMB-4 ensures a high-fidelity representation of the geometry while model EMB-1 introduces an approximation with a 'step' in the thickness of the plate.

As for the case of the surface-mounted sensor, the use of variable kinematic models reduces the computational costs preserving the accuracy of the results.

Surface-mounted VS embedded sensor

The results obtained considering the surface-mounted and the embedded sensors confirm the better performances, in term of effective coupling, of the second solution. The use of embedded sensors allows the loads to be transferred more efficiently to the transducer that is, a higher output voltage can be achieved with the same deformation of the substructure. Figure 12 shows the axial strain field for models SUR-2 and EMB-2.

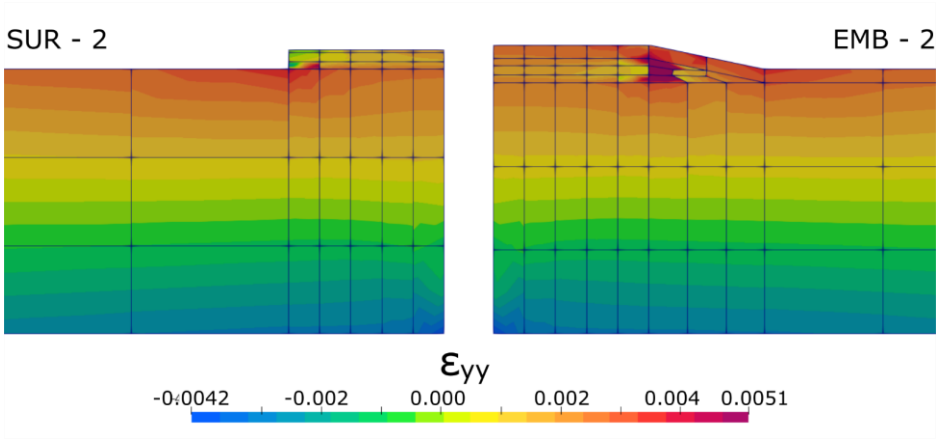

Figure 12 Axial strain field for models SUR-2 and EMB-2

The higher effective coupling factor provided by the embedded sensor can be explained looking at Figure 13 where is reported the axial strain on the upper surface of the piezo patch for models SUR-2 and EMB-2. The results show that the deformation of the embedded sensor is more uniform since no free boundaries are present, as in the case of the surface-mounted sensor.

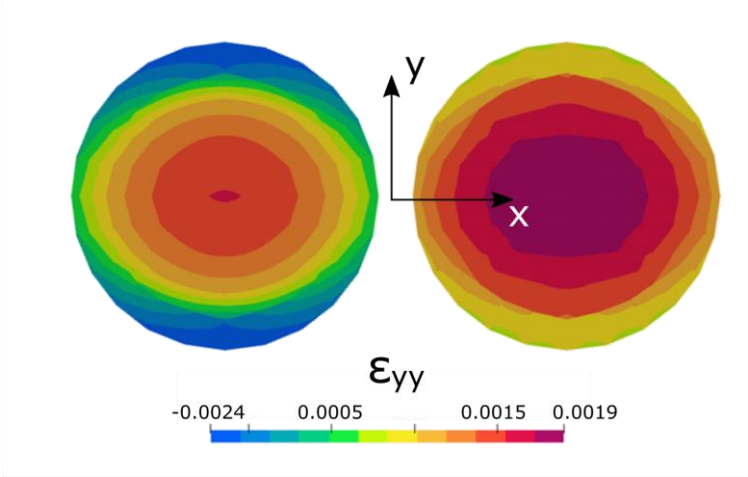

Figure 13 Axial strain on the upper surface of the piezo patch for models SUR-2 and EMB-2. Th

Although the embedded sensor can provide a higher coupling, it should be noted that a strain concentration appears in the adhesive layer, see Figure 12. The presence of a strain concentration could lead to undesired failure or delamination of the structure that

is, a suitable modeling approach should be adopted to predict the reliability of the structure.

Conclusions

An advanced modeling technique for the analysis of smart structures has been presented in the present paper. The Carrera Unified Formulation has been used to derive any order structural theories with an automatic computational tool. The kinematic model has been refined locally by means of the node dependent kinematic approach. The same technique has been used to set compatible kinematics at the interface between elements with different dimensions.

The present global-local framework has been used to investigate layered structures with localized piezoelectric transducers. Different modeling approaches have been compared, and the results have been validated with those from literature. The results suggest the following considerations:

- The use of embedded sensors gives a higher effective coupling factor but can lead to premature failure of the structure due to local stress concentrations.
- A refined modeling approach is mandatory in the analysis of smart structures to represent the interface between the piezo-patch and the hosting structure accurately.
- The use of the present global-local approach can reduce the computational costs keeping the same level of accuracy.

In conclusion, the present approach is very promising for the analysis of smart structures and could find applications in the design of health-monitoring systems. The numerical advantages presented in this paper are expected to be more significant in the

analysis of larger structures. In this case, just a few spots would require a refined model while most of the structure could be solved using the global model.

Bibliography

1. Tang HY, Winkelmann C, Lestari W, La Saponara V. Composite structural health monitoring through use of embedded PZT sensors. J Intell Mater Syst Struct. 2011;22(8):739–55.
2. Su Z, Wang X, Chen Z, Ye L, Wang D. A built-in active sensor network for health monitoring of composite structures. Smart Mater Struct. 2006;15(6):1939–49.
3. Crawley EF, Luis J. Use of piezoelectric actuators as elements of intelligent structures. AIAA J. 1987;(25):1373–85.
4. Benjeddou A. Advances in piezoelectric finite element modeling of adaptive structural elements: a survey. Comput Struct. 2000;76(1):347–63.
5. Al-Ajmi MA, Benjeddou A. Damage indication in smart structures using modal effective electromechanical coupling coefficients. Smart Mater Struct. 2008;17(3).
6. Su Z, Ye L, Lu Y. Guided Lamb waves for identification of damage in composite structures: A review. J Sound Vib. 2006;295(3–5):753–80.
7. Yasin MY, Ahmad N, Alam MN. Finite element analysis of actively controlled smart plate with patched actuators and sensors. Lat Am J Solids Struct. 2010;7:227–47.
8. Reddy JN. On laminated composite plates with integrated sensors and actuators. Eng Struct. 1999;21(7):568–93.
9. Huang Y, Nemat-Nasser S. Structural integrity of composite laminates with

embedded micro-sensors. Sens Syst Networks Phenomena, Technol Appl NDE Heal Monit 2007. 2007;6530:65300W.

10. Shin S, Zamorano B, Elvin N. Comparison of the electromechanical properties of embedded and surface-mounted piezoelectric transducers. J Intell Mater Syst Struct. 2016;27(20):2837–50.
11. Ghasemi-Nejhad MN, Russ R, Pourjalali S. Manufacturing and testing of active composite panels with embedded piezoelectric sensors and actuators. J Intell Mater Syst Struct. 2005;16(2):319–33.
12. Lin M, Chang FK. The manufacture of composite structures with a built-in network of piezoceramics. Compos Sci Technol. 2002;62(7–8):919–39.
13. Konka HP, Wahab MA, Lian K. The effects of embedded piezoelectric fiber composite sensors on the structural integrity of glass-fiber-epoxy composite laminate. Smart Mater Struct. 2012;21(1).
14. Shukla DR, Vizzini AJ. Interlacing for improved performance of laminates with embedded devices. Smart Mater Struct. 1996;5(2):225–9.
15. Chilles JS, Croxford A, Bond IP. Design of an embedded sensor, for improved structural performance. Smart Mater Struct [Internet]. 2015;24(11):115014. Available from: http://dx.doi.org/10.1088/0964-1726/24/11/115014
16. Bowen CR, Watson M, Betts DN, Harris P, Bertin M, Kim HA. Piezoelectric fibres integrated into structural composites. Ferroelectrics. 2014;466(1):14–20.
17. Chee CYK, Tong L, Steven GP. A review on the modelling of piezoelectric sensors and actuators incorporated in intelligent structures. J Intell Mater Syst Struct. 1998;9(1):3–19.
18. Ghasemi H, Park HS, Rabczuk T. A level-set based IGA formulation for topology optimization of flexoelectric materials. Comput Methods Appl Mech

Eng [Internet]. 2017;313:239–58. Available from: http://dx.doi.org/10.1016/j.cma.2016.09.029

19. Nanthakumar SS, Lahmer T, Zhuang X, Zi G, Rabczuk T. Detection of material interfaces using a regularized level set method in piezoelectric structures. Inverse Probl Sci Eng. 2016;24(1):153–76.
20. Sarvanos DA. Mixed laminate theory and finite element for smart piezoelectric composite shell structures. AIAA J. 1997;35:1327–33.
21. Wang J, Yang J. Higher-order theories of piezoelectric plates and applications. Appl Mech Rev. 2000;53(4):87–99.
22. Shu X. Free vibration of laminated piezoelectric composite plates based on an accurate theory. Compos Struct. 2005;67(4):375–82.
23. Tzou HS, Gadre M. Theoretical analysis of a multi-layered thin shell coupled with piezoelectric shell actuators for distributed vibration controls. J Sound Vib. 1989;132(3):433–50.
24. Kulikov GM, Plotnikova S V. Exact {3D} stress analysis of laminated composite plates by sampling surfaces method. Compos Struct. 2012;94(12):3654–63.
25. Beheshti-Aval SB, Lezgy-Nazargah M, Vidal P, Polit O. A refined sinus finite element model for the analysis of piezoelectric-laminated beams. J Intell Mater Syst Struct. 2011;(22):203–10.
26. Robaldo A, Carrera E, Benjeddou A. A unified formulation for Finite Element Analysis of Piezoelectric Plates. Comput {&} Struct. 2006;84(22–23):1494–505.
27. Carrera E, Boscolo M, Robaldo A. Hierarchic multilayered plate elements for coupled multifield problems of piezoelectric adaptive structures: formulation and numerical assessment. Arch Comput methods Eng. 2007;14(4):383–430.
28. Carrera E, Büttner A, Nali P. Mixed elements for the analysis of anisotropic

multilayered piezoelectric plates. J Intell Mater Syst Struct. 2010;21(7):701–17.

29. Kim J, Varadan V V, Varadan VK. Finite element modelling of structures including piezoelectric active devices. Int J Numer Methods Eng. 1997;832:817–32.

30. Srivastava A, Lanza di Scalea F. Quantitative structural health monitoring by ultrasonic guided waves. J Eng Mech. 2010;136(8):937–44.

31. Spada A, Capriotti M, Cui R, Di Scalea FL. Improved global-local model to predict guided-wave scattering patterns from discontinuities in complex parts. In: Proceedings of SPIE - The International Society for Optical Engineering. 2019.

32. Alaimo A, Milazzo A, Orlando C. Global/Local FEM-BEM stress analysis of damaged aircraft structures. C - Comput Model Eng Sci. 2008;36(1):23–41.

33. Carrera E, Cinefra M, Petrolo M, Zappino E. Finite Element Analysis of Structures Through Unified Formulation. John Wiley {&} Sons; 2014.

34. Zappino E, Carrera E. Multidimensional model for the stress analysis of reinforced shell structures. AIAA J. 2018;56(4).

35. Carrera E, Zappino E. One-dimensional finite element formulation with node-dependent kinematics. Comput Struct. 2017;192:114–25.

36. Carrera E, Zappino E, Li G. Analysis of beams with piezo-patches by node-dependent kinematic finite element method models. J Intell Mater Syst Struct [Internet]. 2018;29(7):1379–1393. Available from: https://doi.org/10.1177/1045389X17733332

37. Zappino E, Li G, Pagani A, Carrera E. Global-local analysis of laminated plates by node-dependent kinematic nite elements with variable ESL/LW capabilities. Compos Struct. 2017;172:1–14.

38. Garusi E, Tralli A. A hybrid stress-assumed transition element for solid-to-beam

and plate-to-beam connections. Comput Struct. 2002;80(2):105–15.

39. Chavan KS, Wriggers P. Consistent coupling of beam and shell models for thermo-elastic analysis. Int J Numer Methods Eng [Internet]. 2004;59(14):1861–78. Available from: http://doi.wiley.com/10.1002/nme.938

40. Edery-Azulay L, Abramovich H. Piezoelectric actuation and sensing mechanisms--closed form solutions. Compos Struct. 2004;64(3–4):443–53.